Simulating TeV gamma-ray morphologies of shell-type supernova remnants

Matteo Pais[1]

in collaboration with C. Pfrommer[2], K. Ehlert[2], R. Pakmor[3], M. Werhahn[3], G. Winner[2]

[1] HUJI, [2] AIP Potsdam, [3]MPIA Garching

TeVPA 2023, Napoli, 13th September 2023

Acceleration of Ions at the shock

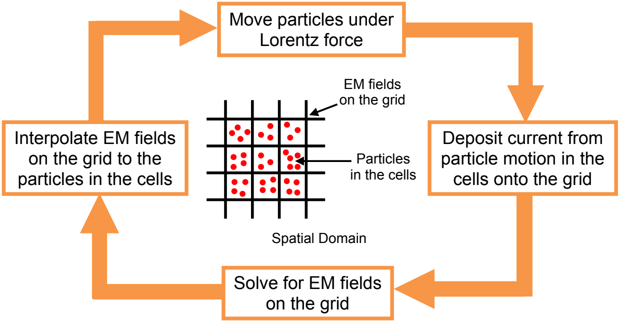

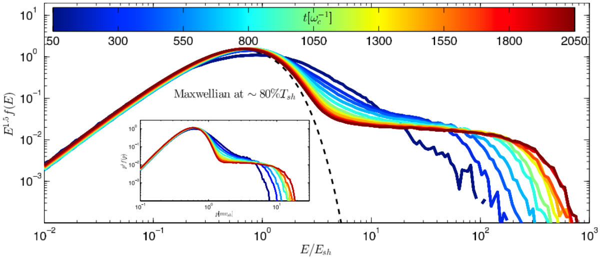

(from Caprioli and Spitkovsky, 2014)

Obliquity-dependent shock acceleration

Quasi-parallel shocks accelerate more efficiently! Magnetic obliquity: $\cos\theta = \hat{\mathbf{n}}_s \cdot \hat{\mathbf{b}}$

$$\zeta(\theta) \simeq \frac{\zeta_0}{2}\left[\tanh\left(\frac{\theta_{crit} - \theta}{\delta}\right) + 1\right]$$

with $\zeta_0 \simeq 15\%$, $\theta_{crit} = 45^\circ$

- efficient **quasi-parallel** acceleration
- inefficient **quasi-perpendicular** acceleration

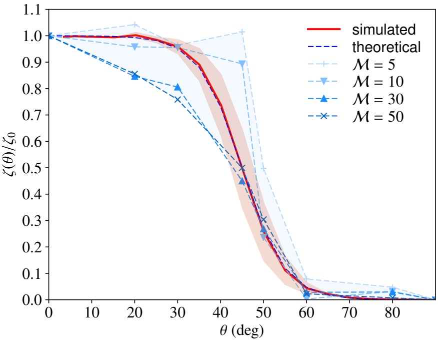

Functional dependence of the CR acceleration efficiency on the magnetic obliquity angle from hybrid PIC simulations of non-relativistic shocks (Caprioli & Spitkovsky, 2014a, Pais et al. 2018).;

AREPO (Springer, 2010) is a massive parallel code in which the gas physics is calculated on a moving Voronoi irregular mesh.

- full 3D simulations with ideal MHD;
- shock finder method (Schaal & Springer 2015, Pfrommer et al. 2017)
- Mach number $\mathcal{M}$ and magnetic obliquity θ are calculated at each shocked cell;
- CR injection at the shock;
- CRs are added as a second, relativistic fluid ($\gamma = 4/3$) next to the thermal gas ($\gamma = 5/3$) and evolved according to the advection-diffusion equation:

$$\frac{\partial \varepsilon_{\rm cr}}{\partial t} + \boldsymbol{\nabla} \cdot [\varepsilon_{\rm cr} \boldsymbol{v} - \kappa_\varepsilon \boldsymbol{b}(\boldsymbol{b} \cdot \boldsymbol{\nabla} \boldsymbol{\varepsilon}_{\rm cr})] = -P_{\rm cr} \boldsymbol{\nabla} \cdot \boldsymbol{v} + \underbrace{\Lambda_{\rm cr}}_{\rm losses} + \underbrace{\Gamma_{\rm cr}}_{\rm gains}$$

Closure relation:

$$P_{\rm cr} = (\gamma - 1)\varepsilon_{\rm cr}$$

Pfrommer et al., 2017

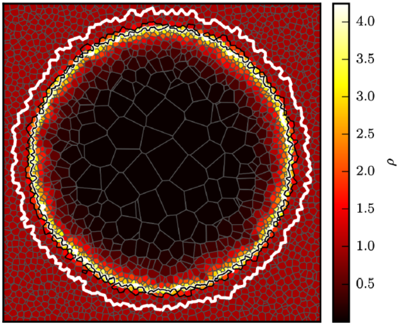

Point explosions with CR injection at shocks. Uniform $\boldsymbol{B}$ field

Pais et al, 2018

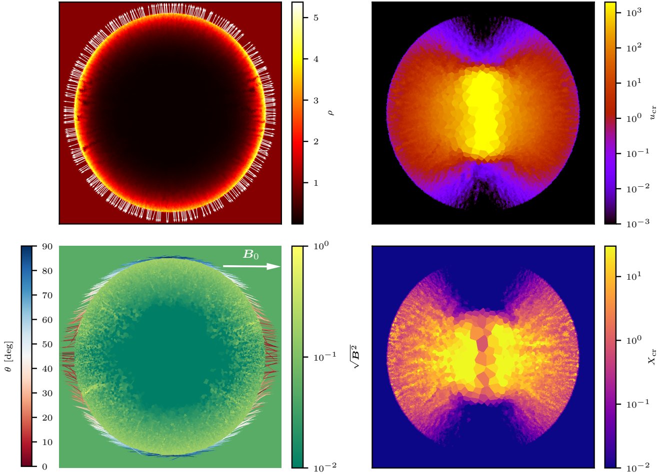

- CR acceleration with homogeneous magnetic field
- oblation of the shock in correspondence of CR efficient acceleration

Point explosions with CR injection at shocks. Uniform vs turbulent $\boldsymbol{B}$

Pais et al, 2018

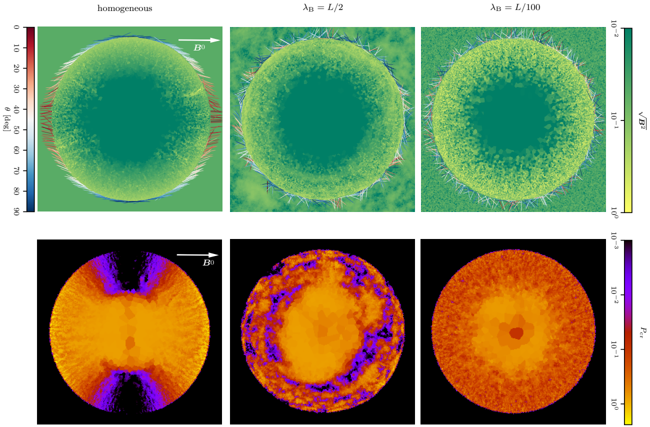

- turbulent magnetic field with Kolmogorov power spectrum $P(k) \propto (k/k_{\rm inj})^{-11/3}$ with different coherence lengths $\lambda_B = 2\pi/k_{\rm inj}$.
- $\langle\zeta\rangle \simeq 0.3\zeta_0 \simeq 5\%$ for all cases.
- we can apply these results to reproduce the TeV emission of young SNR.

The interaction of CRs with matter and photon fields generates a **multi-wavelength spectrum:**

- **hadronic interactions** $(\mathrm{pp}, \mathrm{p}\alpha, \alpha\mathrm{p})$ (neutral pion decay)
- **leptonic processes**: synchrotron, bremsstrahlung, inverse Compton scattering

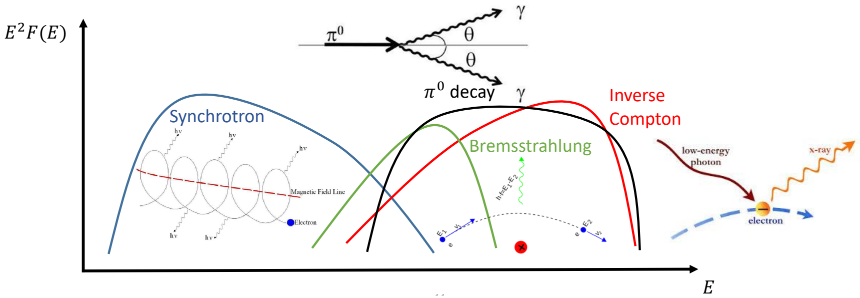

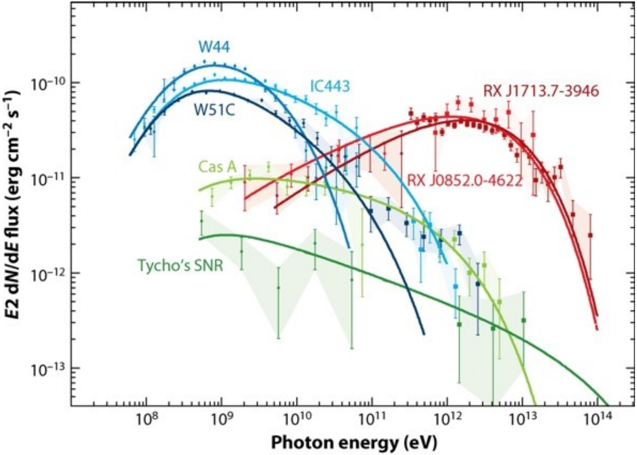

Funk, 2015

TeV spectrum slope $\alpha \gtrsim 2$ + cutoff at 50-200 TeV

Matching of TeV gamma-ray spectra + flux + emission morphology

- TeV Gamma-ray flux $\mathcal{F}_\gamma$ of SNR for the hadronic model ($>$ TeV) (Gabici & Aharonian, 2016) integrated yields

$$\mathcal{F}_\gamma \simeq 2.7 \times 10^{-12} \left(\frac{W_\mathrm{p}}{10^{50}\,\mathrm{erg}}\right) \left(\frac{n}{0.1\,\mathrm{cm}^{-3}}\right) \left(\frac{D}{1\,\mathrm{kpc}}\right)^{-2} \frac{\mathrm{ph}}{\mathrm{cm}^2\ \mathrm{s}}.$$

- Sedov solution:

$$r_\mathrm{ST}(t) = \left(\frac{E_\mathrm{SN}}{\alpha\rho}\right)^{1/5} t_\mathrm{age}^{2/5},$$

- $\mathcal{F}_\gamma$ + Sedov-Taylor solution $\longrightarrow$ for given W_p, $\mathcal{F}_\gamma$, θ, constraints on n, D, t_age
- We assume in post-processing a CR distribution based on simulated P_cr:

$$f^{1\mathrm{D}}(p_i) = \frac{\mathrm{d}^2 N_i}{\mathrm{d}p_i \mathrm{d}V} \propto p_i^{-\alpha_i} \exp\left[-\left(\frac{p_i}{p_{i,\mathrm{cut}}}\right)^{\beta_i}\right]$$

- synthetic hadronic TeV-γ ray maps + instrumental noise modeling + PSF convolution.
- **Morphology and the patchiness of the emission give constraints on the coherence scale of the magnetic field λ_B.**

We chose gamma-ray bright shell-type and bi-lobed SNRs:

SN 1006 (bi-lobed):

- location at 0.5 kpc above the galactic plane;
- uniform ISM density (possible large scale density gradient ∇n)
- mainly **constant magnetic field** (large scale coherence scale)

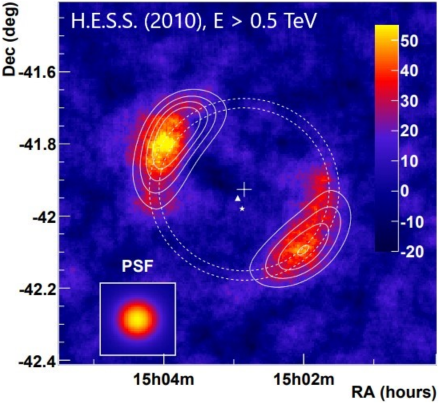

Vela Jr. and **RX-J1713** (both shell-type)

- Core collapse SN progenitor in star forming region;
- **turbulent magnetic field** (models with different λ_B);
- low density cavity inferred from lack of thermal X-ray emission (Slane, 2001), dense clouds are observed ($n \sim 10^2 \mathrm{cm}^{-3}$) (Fukui et al, 2017)
- clouds break into small clumps $n_c \simeq 10^4 \mathrm{cm}^{-3}$ (Inoue, 2012, Celli 2019)
- we simulate 7000 clumps with $n_c = 10^3 \mathrm{cm}^{-3}$, $R_c = 0.1$ pc for $M_{c,\mathrm{tot}} = 50 M_\odot$

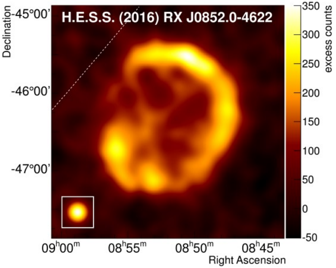

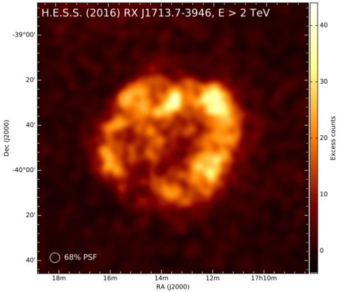

Uniform and clumpy medium compared

Pais et al., 2020

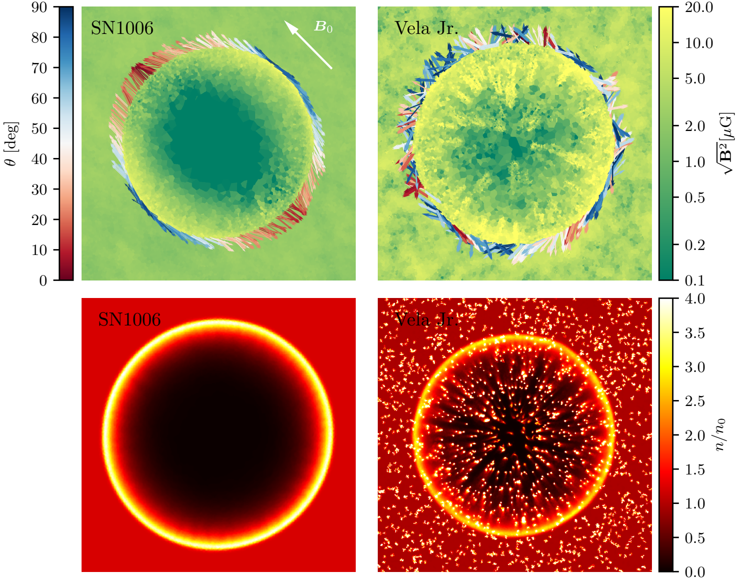

Pais et al. (2020)

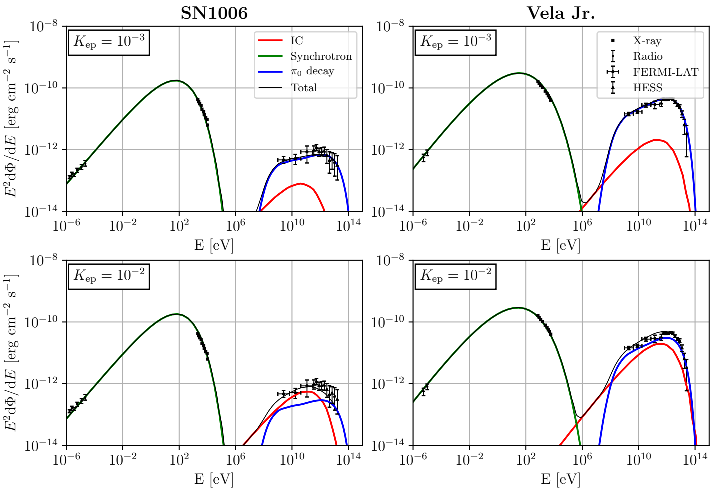

Multi-frequency spectra of SN1006 (left-hand panels) and Vela Jr. (right-hand panels). The top panels show a hadronic scenario for both remnants assuming an electron-to-proton ratio of $K_{ep} = 10^{-3}$. The bottom panels show a mixed hadronic-leptonic scenario with $K_{ep} = 10^{-2}$.

How the different magnetic field morphology shapes the emission.
The cases of SN1006 ($\boldsymbol{B}$ = const., from NW to SE) and Vela Jr. (turbulent $\boldsymbol{B}$)

Pais et al., 2020

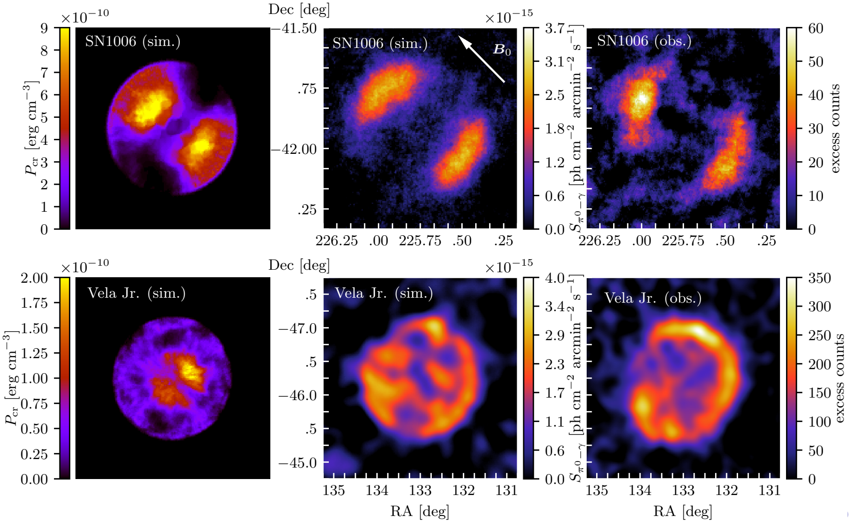

Pais & Pfrommer, 2020

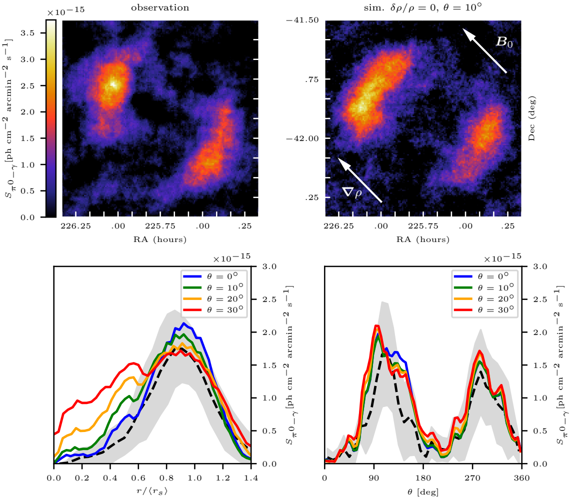

Large scale density gradient modulates the different brightness of the NE and SW poles ($\nabla n = (3.4 \pm 0.2) \times 10^{-3}\mathrm{cm}^{-3}\mathrm{pc}^{-1}$)

Modeling TeV gamma-ray emission from shell-type SNRs. B-field coherence scale

Pais & Pfrommer, 2020

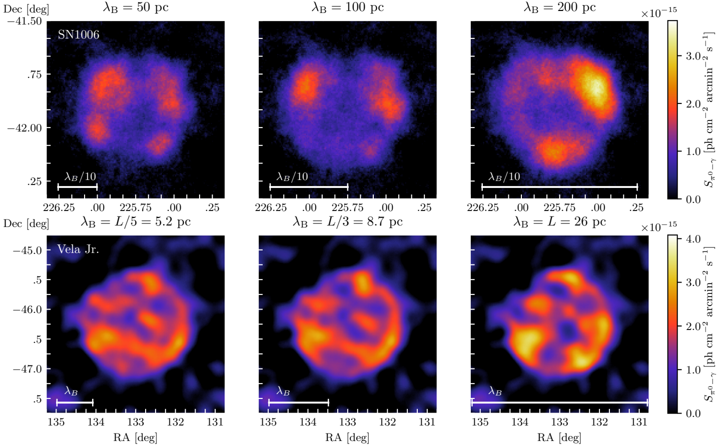

Correlation structure of patchy TeV -rays constrains magnetic coherence scale in ISM:

$$\text{SN1006: } \lambda_B > 200^{+50}_{-40} \text{ pc, Vela Jr.: } \lambda_B \simeq 13^{+13}_{-4.3} \text{ pc}$$

Pais & Pfrommer, 2020

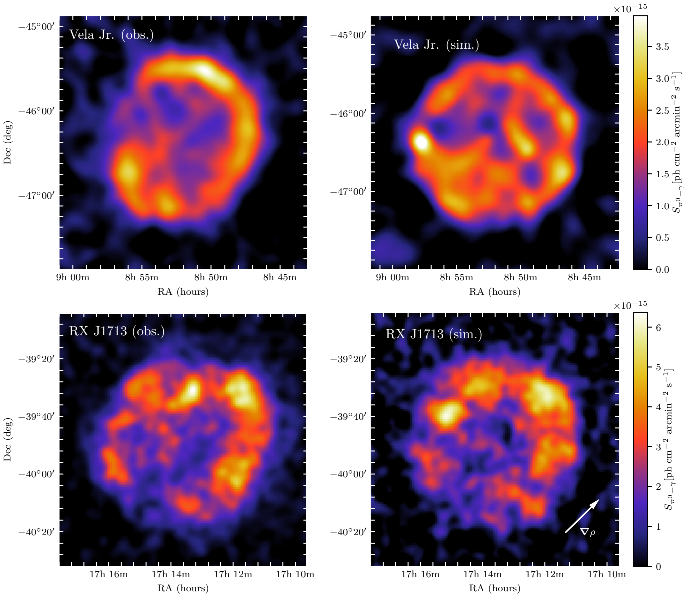

Pais & Pfrommer, 2020

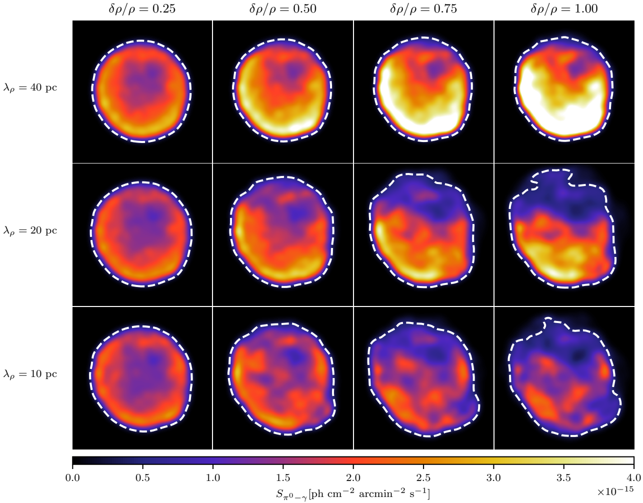

Can density fluctuations explain the TeV brightness variability?

Pais & Pfrommer, 2020

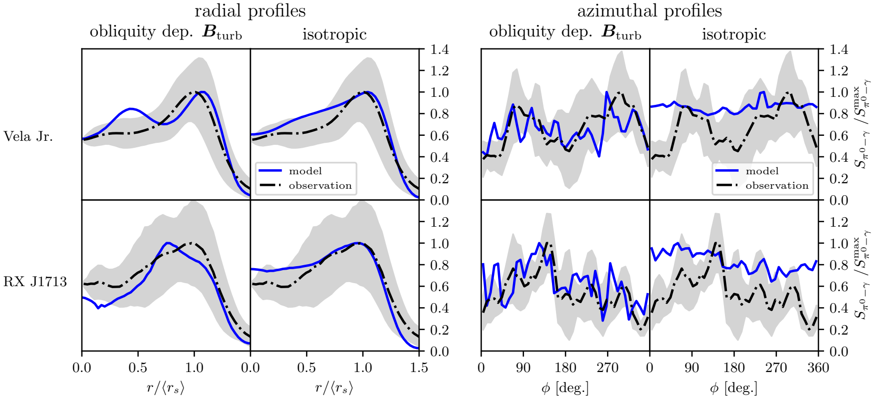

- anisotropy of corrugated shock surfaces limits (large-scale) density fluctuations to $\delta\rho/\rho < 0.75$
- only obliquity-dep. acceleration explains patchy TeV gamma-ray emission

Conclusions

- Obliquity-dependent shock acceleration predicts an average CR efficiency of $\sim 5\%$ per SNR;
- Hadronic CR population is able to match TeV gamma-ray emission flux and high-energy spectra for the analyzed SNRs using a 1-zone model;
- Low hadronic emission from low density ISM environment can be reinforced by small dense clumps distributed in the ISM;
- Full 3D MHD simulations with obliquity depenent CR shock acceleration reproduce the patchy and bi-lobed emission from SNRs for different $\mathbf{B}$ field topology in a single simple model;
- Prediction of the coherence scale of the local magnetic field using the SNR emission morphology
- Density fluctuations only in isotropic injection models are unable to reproduce the filamentous emission;

Extra

Pais et al., 2020

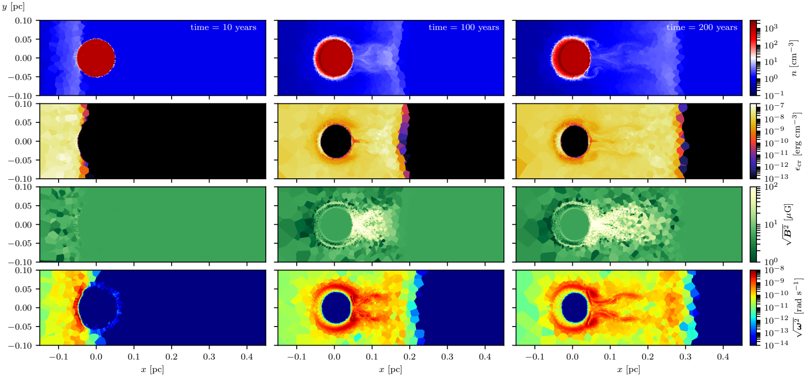

- Shock is slowed down inside the clumps $v_s \propto v_{s,0}/\sqrt{\delta}$ where $\delta = \rho_{\rm clump}/\rho_0$
- only high-energy CRs can penetrate the clumps;
- not all the clumped material is accelerated at once;
- clump-blastwave interaction injects vorticity in the system;
- semi-analytic model to the contribution of a population of clumps to the total gamma-ray luminosity.

There are two concurrent scenarios to explain the high-energy gamma-ray emission from SNRs:

- **leptonic**: inverse Compton scattering on CMB photons or starlight (assuming $n(\gamma)_{\mathrm{e}} \propto \gamma^{-\alpha}$):

$$P_{w,\mathrm{IC}}(E_1) \propto \frac{3\sigma_{\mathrm{T}} c}{(hc)^3} E_1^{-\frac{\alpha-1}{2}} (kT)^{\frac{\alpha+5}{2}}$$

- **hadronic**: $\mathrm{pp}, \mathrm{p}\alpha, \alpha\mathrm{p}$ interactions

$$\begin{cases} \pi^{\pm} \to \mu^{\pm} + \nu_{\mu}/\bar{\nu}_{\mu} \to e^{\pm} + \nu_e/\bar{\nu}_e + \nu_{\mu} + \bar{\nu}_{\mu} \ , \\ \pi^0 \to \gamma\gamma \ . \end{cases}$$

Analytical approximation of the source function (assuming $f_{\mathrm{p}}(E_{\mathrm{p}}) \propto E_{\mathrm{p}}^{-\alpha}$) (Pfrommer & Ensslin, 2004):

$$q_{\pi^0}(E_{\pi}) \propto \sigma_{\mathrm{pp}} n_{\mathrm{N}} c \left(\frac{2E_{\pi}}{\mathrm{GeV}}\right)^{-\alpha}$$